Electronic Supporting Information

for

Yellow-emissive carbon nanodot-based ratiometric fluorescent nanosensor for visualization of exogenous and endogenous hydroxyl radicals in mitochondria of live cells

Danling Zhou [1], Hong Huang [2,*], Yangang Wang [2,*], Yan Wang [1,*], Zuming Hu [1], Xi Li [2]

[1] College of Materials Science and Engineering, Donghua University, Shanghai 201620, China.

[2] College of Biological, Chemical Sciences and Engineering, Jiaxing University, Jiaxing 314001, China.

*Corresponding author:

huangho17@163.com (*H. Huang*);

ygwang8136@mail.zjxu.edu.cn(*Y. Wang*);

wy@dhu.edu.cn (*Y. Wang*).

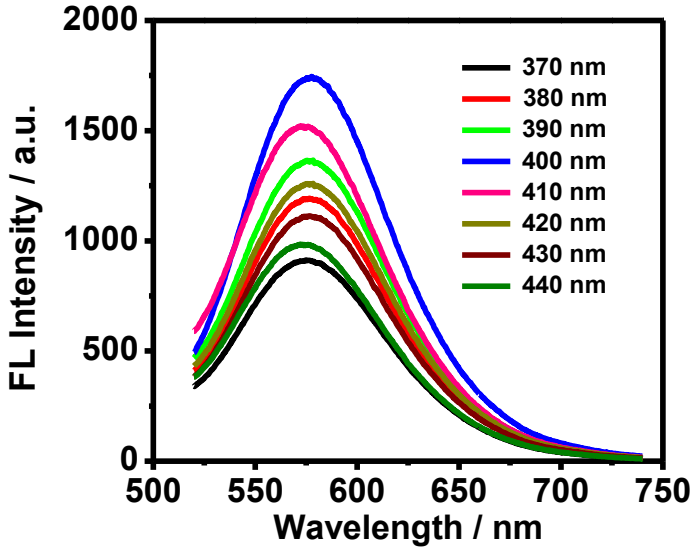

Fig. S1 Fluorescence spectra of the CDs obtained under different excitation wavelength from 370 to 440 nm.

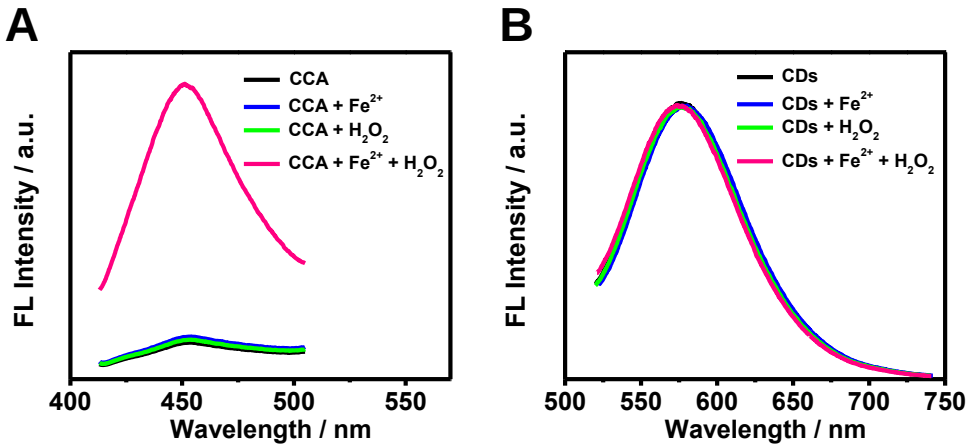

Fig. S2 Fluorescence responses of (A) CCA and (B) CDs to 100 μM Fe^{2+}, 1 mM H_2O_2, and 100 μM •OH.

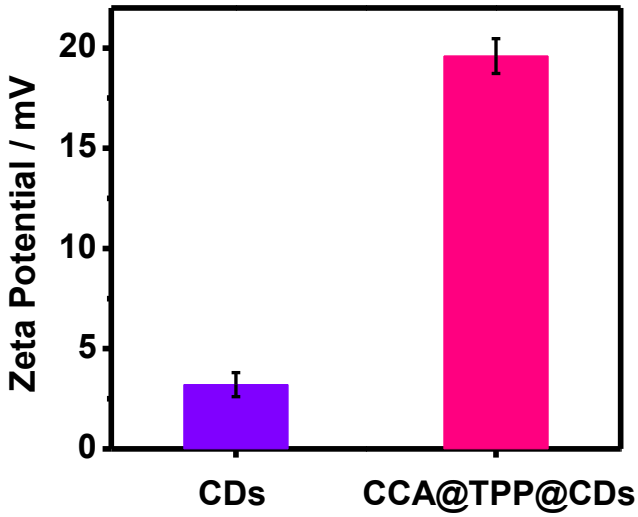

Fig. S3 Zeta potentials of CDs and the CCA@TPP@CDs nanosensor. Zeta potentials of CDs and the CCA@TPP@CDs nanosensor were recorded at a concentration of 60 μg mL^{-1} in aqueous solution.

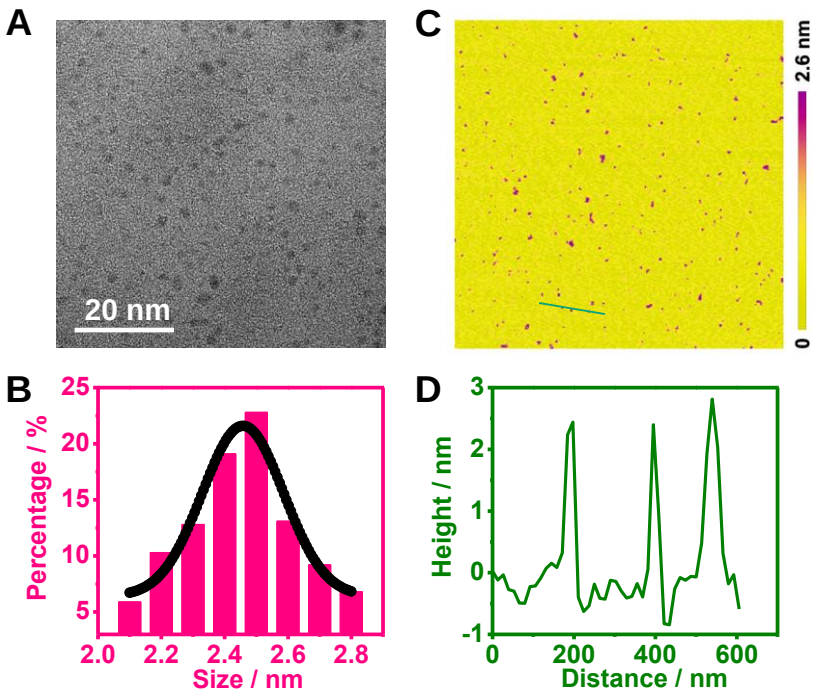

Fig. S4 (A) Typical TEM image of the nanosensor. (B) The corresponding size-distribution histogram. (C) Representative AFM image of the nanosensor. (D) The height distribution of the nanosensor along the line.

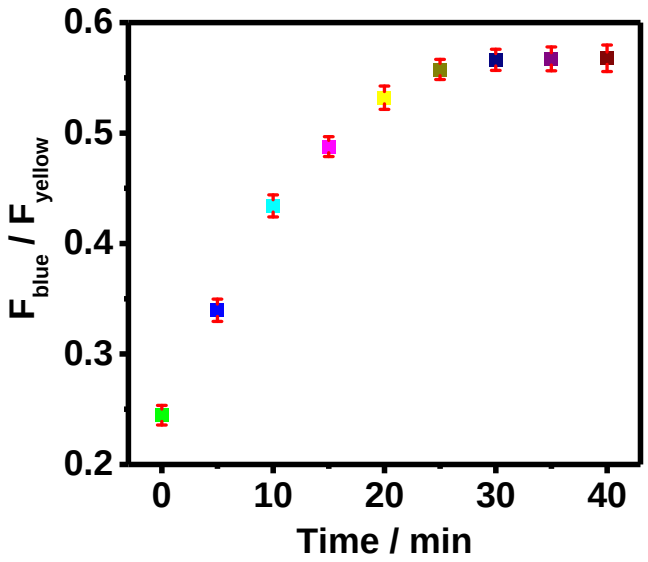

Fig. S5 Time dependence of the fluorescence ratio of the nanosensor (60 μg/mL) in the presence of 100 μM •OH.

Table S1 Comparison of the performances of different fluorescent methods for the determination of •OH.

FL method	Linear range (μM)	LOD (μM)	Manner	Ref.
Cyanine-based fluorochrome	0 - 60	0.038	Single intensity	S1
Citrate-capped CdTe QDs	0.1 - 100	-	Single intensity	S2
MPT-Cy2	1 - 10	1.16	Single intensity	S3
AuNC@HPF	1 - 150	0.68	Ratiometric	S4
Si QDs−Ce6	1 - 200	0.97	Ratiometric	S5
Uniform Materials Based on Organic Salts	0 - 25	0.769	Ratiometric	S6
CCA@TPP@CDs	0.1 - 160	0.070	Ratiometric	This work

References

S1. H. Li, X. Li, W. Shi, Y. Xu and H. Ma, *Angew. Chem. Int. Ed.*, 2018, **57**, 12830-12834.

S2. W. Zhou, Y. Cao, D. Sui and C. Lu, *Angew. Chem. Int. Edit.*, 2016, **55**, 4236-4241.

S3. F. Liu, J. Du, D. Song, M. Xu and G. Sun, *Chem. Commun.*, 2016, **52**, 4636-4639.

S4. M. Zhuang, C. Ding, A. Zhu and Y. Tian, *Anal. Chem.*, 2014, **86**, 1829-1836.

S5. Q. Zhao, R. Zhang, D. Ye, S. Zhang, H. Chen and J. Kong, *ACS Appl. Mater. Interfaces*, 2017, **9**, 2052-2058.

S6. M. Cong, N. Siraj, N. Bhattarai, P. E. Kolic, K. S. McCarter, P. K. Chhotaray and I. M. Warner, *Sens. Actuators B: Chem.*, 2018, **257**, 993-1000.

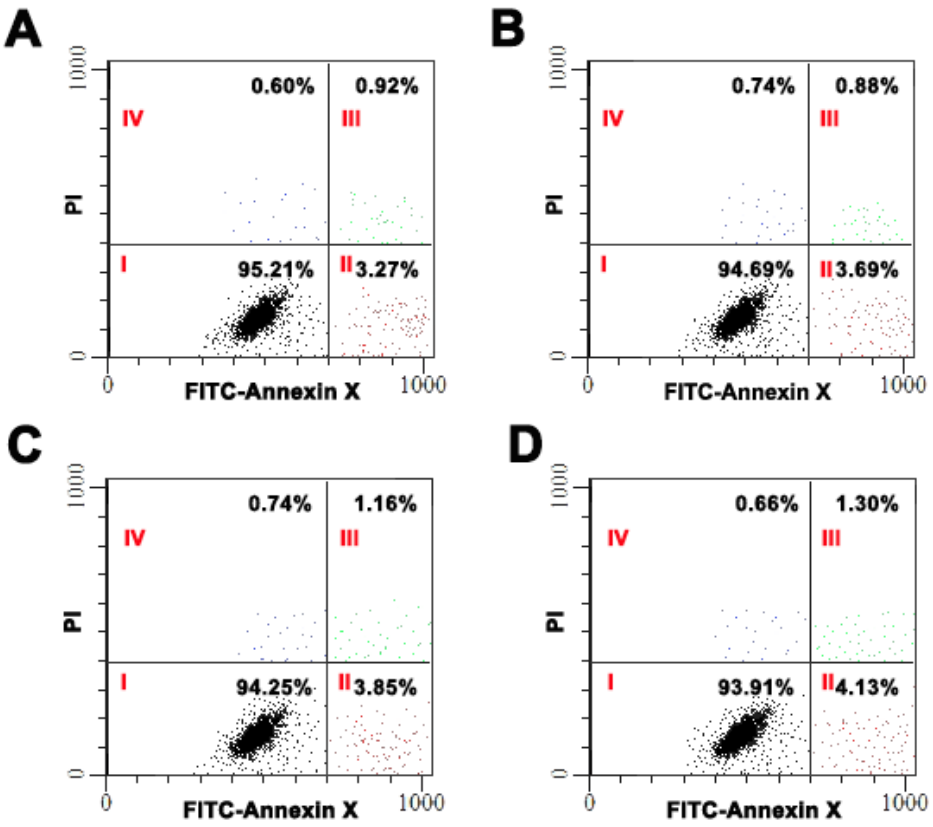

Fig. S6 Apoptosis assay of RAW264.7 cells incubated with the nanosensor at concentrations of (A) 0 μg/mL, (B) 40 μg/mL, (C) 80 μg/mL, and (D) 120 μg/mL. I, II, III, and IV respectively represent the region of normal cells, early apoptotic cells, late apoptotic cells, and dead cells.

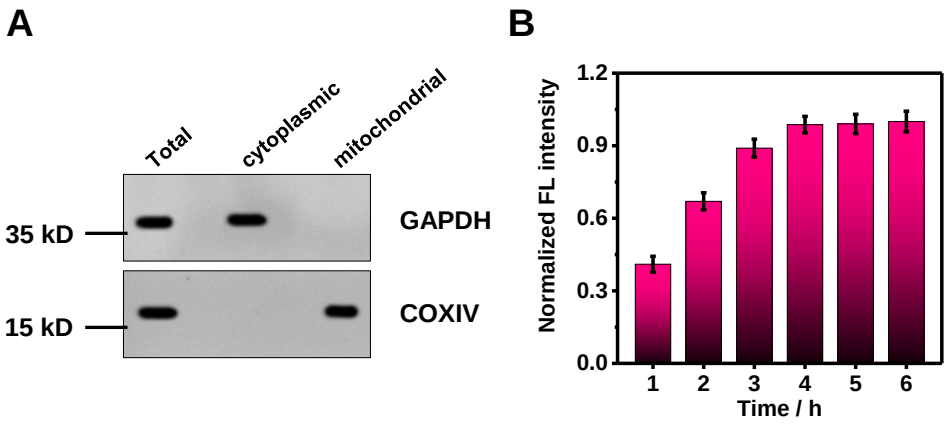

Fig. S7 (A) Immunoblotting analysis of relative levels of GAPDH (cytoplasmic marker) and COXIV (mitochondrial marker) in cytoplasmic and mitochondrial fractions purified from cells. (B) Fluorescence intensity changes of the PBS solution containing isolated mitochondria.

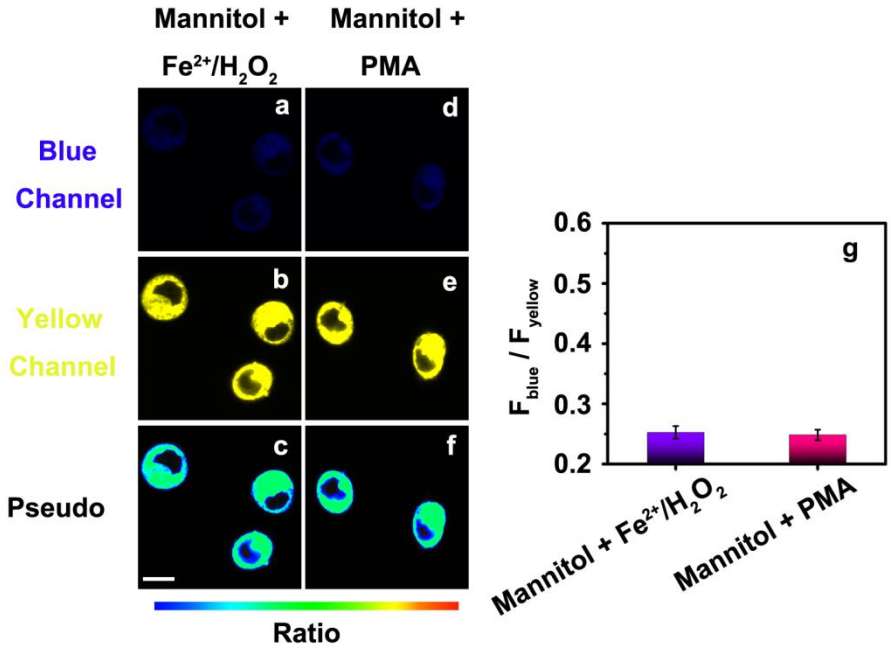

Fig. S8 Fluorescence images of RAW264.7 cells under different treatments. (a, b, c) Fluorescence images of RAW264.7 cells that were treated with the nanosensor (60 μg/mL), mannitol (10 mM), and •OH (100 μM, generated from Fe^{2+}/H_2O_2 system) in order. (d, e, f) Fluorescence images of RAW264.7 cells that were treated with the nanosensor (60 μg/mL), mannitol (10 mM), and PMA (2.0 μg/mL) in sequence. (a, d) Fluorescence images from the blue channel (λ_{em} = 420-500 nm). (b, e) Fluorescence images from the yellow channel (λ_{em} = 530-610 nm). (c, f) Pseudo-colored ratio images obtained from the blue and yellow channels. (g) The corresponding F_{blue}/F_{yellow}. Data are represented as mean ± s.d. of 40 cells. Scale bar: 10 μm.